Journal of Solid State Chemistry 181 (2008) 2298–2305

Contents lists available at ScienceDirect

Journal of Solid State Chemistry

journal homepage: www.elsevier.com/locate/jssc

Characterization of CoMCM-41 mesoporous molecular sieves obtained by the microwave irradiation method

Tingshun Jiang [a,*], Wei Shen [a], Qian Zhao [a], Mei Li [a], Jinyu Chu [b], Hengbo Yin [a]

[a] School of Chemistry and Chemical Engineering, Jiangsu University, Jiangsu Province 212013, PR China
[b] School of Environment, Jiangsu University, Jiangsu Province 212013, PR China

ARTICLE INFO

Article history:
Received 9 December 2007
Received in revised form
3 May 2008
Accepted 7 May 2008
Available online 15 May 2008

Keywords:
CoMCM-41 mesoporous molecular sieve
Microwave irradiation method
Characterization
Stability
Synthesis

ABSTRACT

CoMCM-41 mesoporous molecular sieves with different amounts of cobalt were synthesized via the microwave irradiation method. The samples were characterized by X-ray diffraction (XRD), Fourier transform infrared (FT-IR), temperature programmed reduction (TPR), transmission electron microscopy (TEM) and N_2 adsorption–desorption technique, and thermal and hydrothermal stabilities of synthesized CoMCM-41 samples were also investigated. Results show that these synthesized materials have typical mesoporous structure of MCM-41. Also, specific surface area and pore volume of synthesized CoMCM-41 decrease with increasing amount of cobalt added, and mesoporous ordering also decreases. When the molar ratio of SiO_2:CoO in the starting material is 1.0:0.05, mesoporous ordering of synthesized CoMCM-41 is the best among the four doping contents. On the other hand, results of thermal and hydrothermal tests show that CoMCM-41 after calcination at 750 °C for 3 h or hydrothermal treatment at 100 °C for 5 days still retains mesostructure. However, mesoporous framework is entirely damaged after calcination at 850 °C for 3 h.

1. Introduction

The discovery of a series of mesoporous molecular sieves in 1992 by researchers of Mobil Company [1], opened a new era for researchers looking for nearly ideal materials to bridge the gap between microporous and macroporous materials. As a member of M41S family, MCM-41 mesoporous molecular sieve, with high specific surface area and unique pore structure, has received considerable interest among researchers. Various kinds of mesoporous molecular sieves have been synthesized by different methods [2–6], and a series of metal ions were introduced into the framework of mesoporous molecular sieves [7–13]. Recently, cobalt-containing mesoporous molecular sieve has attracted worldwide attention because of their wide applications in various kinds of catalytic reactions [14–21]. Lim et al. [14] and Jentys et al. [22] synthesized CoMCM-41 with different pore sizes by the hydrothermal method using amines with different alkyl chain lengths as templates and characterized their physicochemical properties. Lim et al. [23] synthesized Co-MCM-41 mesoporous molecular sieve with hexagonal structure by accurately controlling pH value, and the metal oxide on the surface of mesoporous molecular sieve was removed under mild acidic condition. Song et al. [17] and Panpranot et al. [19] loaded Co–Mo or Co–Ru onto MCM-41 mesoporous molecular sieve by the impregnation method and investigated their catalytic properties. Ciuparu et al. [20,21] synthesized Co-MCM-41 with different pore sizes by the hydrothermal method using amines with different alkyl chain lengths as templates, and prepared single-walled carbon nanotubes using CO as a raw material and using the as-synthesized Co-MCM-41 as catalyst. Most of the mesoporous molecular sieves were hydrothermally synthesized in the previously reported literatures [24–30]. The hydrothermal synthesis process needs a long crystallization time and a high crystallization temperature. Compared with the hydrothermal synthesis method, the microwave irradiation technique, taking of microwave dielectric heating, even heating or molecular selective heating, homogeneously and momentarily elevates the temperature of integral synthesis system to crystallization temperature, resulting in more homogeneous nucleation and rapid crystallization [31–33]. At present, microwave irradiation technique is widely applied to the synthesis of mesoporous molecular sieve [34–37], but most investigations aimed at synthesizing pure silica MCM-41 mesoporous molecular sieve. Study on MCM-41 mesoporous molecular sieve with transition metal ions synthesized under microwave irradiation was seldom systematically reported. After introducing transition metal ions into the framework of pure silica MCM-41 mesoporous molecular sieve, the specific surface area and average pore size can be changed and the application in catalytic reaction can also be further extended [17,38].

* Corresponding author. Fax: +86 511 88791708.
E-mail address: tshjiang@ujs.edu.cn (T. Jiang).

0022-4596/$ - see front matter © 2008 Elsevier Inc. All rights reserved.
doi:10.1016/j.jssc.2008.05.010

For this purpose, the synthesis of CoMCM-41 mesoporous molecular sieve was carried out under microwave irradiation condition, and the thermal and hydrothermal stabilities of these synthesized mesoporous materials were investigated in the research work.

2. Experimental

2.1. Materials

Chemicals used in the present work, such as sodium silicate ($Na_2SiO_3 \cdot 9H_2O$), cobalt chloride ($CoCl_2 \cdot 6H_2O$), cetyltrimethyl ammonium bromide (CTAB), and concentrated sulfuric acid (H_2SO_4), all analytical reagent grade, were purchased from Shanghai Chemical Reagent Corporation, PR China.

Table 1
Material proportions (molar ratios) of samples CoMCM-41(X^a) and Si/Co molar ratios of samples CoMCM-41(X^a) after calcination at 550 °C

Samples	$n(SiO_2)$:n(CTAB):n(CoO):$n(H_2O)$	Si/Co
CoMCM-41(a)	1:0.2:0.05:70	1:0.048
CoMCM-41(b)	1:0.2:0.10:70	1:0.094
CoMCM-41(c)	1:0.2:0.15:70	1:0.142
CoMCM-41(d)	1:0.2:0.20:70	1:0.189

[a] $X = a$, b, c and d, respectively.

2.2. Synthesis of CoMCM-41 mesoporous molecular sieves

The synthesis of CoMCM-41 mesoporous molecular sieves was carried out by the microwave irradiation method. According to material proportion in Table 1, a typical synthesis procedure was described as follows: first, a given amount of $CoCl_2 \cdot 6H_2O$ was dispersed into 30 ml distilled water, 28.42 g of sodium silicate ($Na_2SiO_3 \cdot 9H_2O$) was dispersed into 50 ml distilled water, and 7.29 g of CTAB was dispersed into 46 ml distilled water until a gelatinous solution was obtained, and then sodium silicate ($Na_2SiO_3 \cdot 9H_2O$) solution was added into cobalt chloride solution under stirring. The resulting mixture was slowly added into the gelatinous solution under vigorous stirring for 10 min and the pH value of the mixed solution was adjusted to 11 by dropwise addition of sulfuric acid (5 mol/L). After stirring for 80 min again, the resulting suspension was transferred into a 250 ml round-bottomed flask, and then the round-bottomed flask was placed into a microwave oven with a refluxing condenser and heated at boiling point for 2.5 h under continuous microwave irradiation with a power of 220 W (National NN-S570MFS). After cooling to room temperature, the sample was filtered, washed with deionized water, and dried at 120 °C for 24 h to obtain a dried sample [designated as s-CoMCM-41(X)], X is the sample number (Table 1). The s-CoMCM-41(X) sample was heated to 550 °C at a heating rate

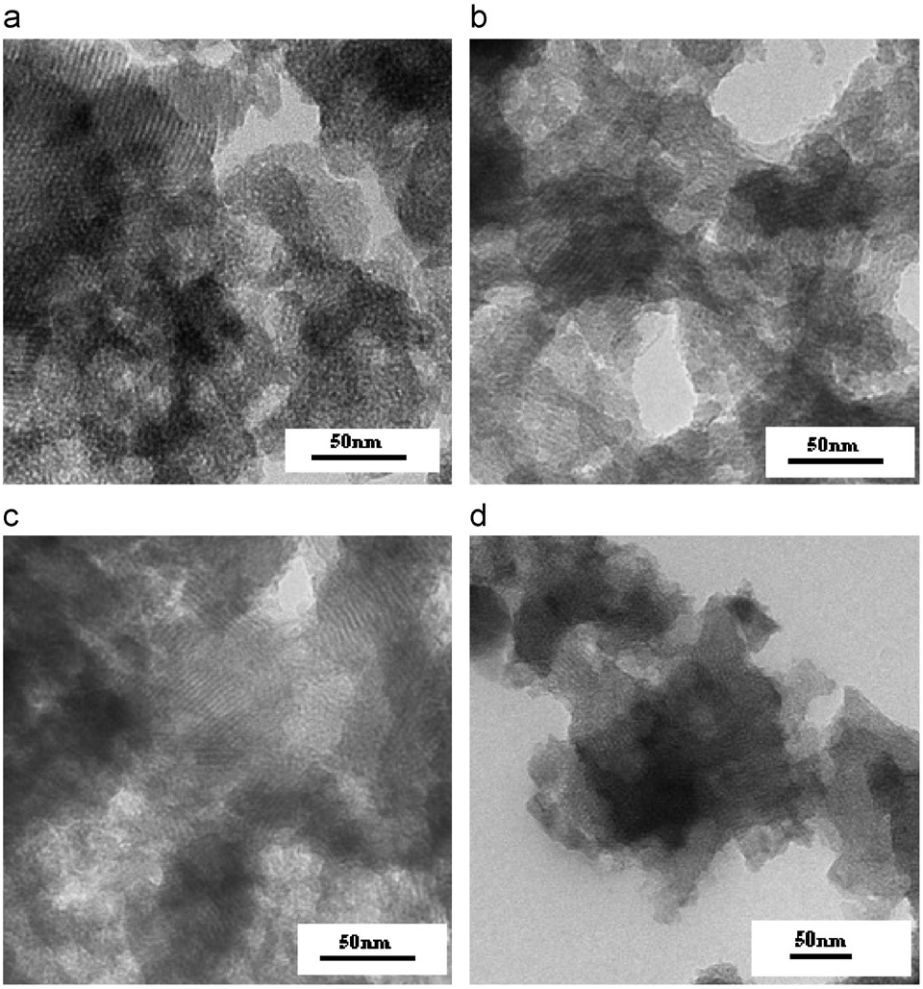

Fig. 1. TEM images of the synthesized samples after calcination at 550 °C.

of 2 °C/min and calcined at 550 °C for 10 h. The calcined sample was designated as CoMCM-41(*X*)-550. The Si/Co molar ratios of the samples determined by chemical analysis are listed in Table 1.

For comparison, the synthesis of CoMCM-41 mesoporous molecular sieve was also carried out via the hydrothermal method according to the molar ratio (SiO_2:CTAB:CoO:H_2O) of 1:0.2:0.10:70. The synthesis procedure was described as following: first, 2.38 g of $CoCl_2 \cdot 6H_2O$ was dispersed into 30 ml distilled water, 28.42 g of sodium silicate ($Na_2SiO_3 \cdot 9H_2O$) was dispersed into 50 ml distilled water, and 7.29 g of CTAB was dispersed into 46 ml distilled water until a gelatinous solution was obtained, and then sodium silicate ($Na_2SiO_3 \cdot 9H_2O$) solution was added into cobalt chloride solution under stirring. The resulting mixture was slowly added into the gelatinous solution under vigorous stirring for 10 min and the pH value of the mixed solution was adjusted to 11 by dropwise addition of sulfuric acid (5 mol/L). After stirring for 80 min again, the resulting suspension was transferred into a 100 ml Teflon-lined stainless steel autoclave and crystallized at 130 °C for 48 h in an oven. After cooling to room temperature, the sample was filtered, washed with deionized water, and dried at 120 °C for 24 h to obtain a dried sample. The dried sample was heated to 550 °C at a heating rate of 2 °C/min and calcined at 550 °C for 10 h, designated as H-CoMCM-41-550.

2.3. Thermal and hydrothermal stability tests

For thermal stability test, the sample CoMCM-41(*X*)-550 was calcined at 650, 750 and 850 °C for 3 h, respectively, designated as CoMCM-41(*X*)-650, CoMCM-41(*X*)-750 and CoMCM-41(*X*)-850, correspondingly. For hydrothermal stability test, 0.5 g of CoMCM-41(*X*)-550 was, respectively, added into a 100 ml Teflon-lined stainless-steel autoclave containing 80 ml of H_2O hydrothermally treated at 100 °C for 3 or 5 days. The hydrothermally treated samples were designated as CoMCM-41(*X*)-3d and CoMCM-41(*X*)-5d, correspondingly.

Thermal and hydrothermal stability tests of the sample H-CoMCM-41-550 were also performed according to the same method. The obtained samples were designated as H-CoMCM-41-650, H-CoMCM-41-750, H-CoMCM-41-3d and H-CoMCM-41-5d, respectively.

2.4. Characterization

The XRD patterns of samples were recorded by using a powder X-ray diffraction instrument (Rigaku D/MAX 2500PC) with Cu $K\alpha$ radiation ($\lambda = 0.15418$ nm). The measurement conditions of XRD are: 40 kV, 50 mA, the scanning range is 1–10° and the scanning speed 1°/min. Specific surface area and pore size were measured by using a NOVA2000e analytical system made by Quantachrome Corporation (USA). Fourier transform infrared (FT-IR) spectra of samples were recorded with a Nexus FT-IR470 spectrometer made by Nicolet Corporation (USA) with KBr pellet technique. The effective range was from 400 to 4000 cm^{-1}. The specific surface area was calculated by the Brunauer–Emmett–Teller (BET) method. Pore size distribution and pore volume were calculated

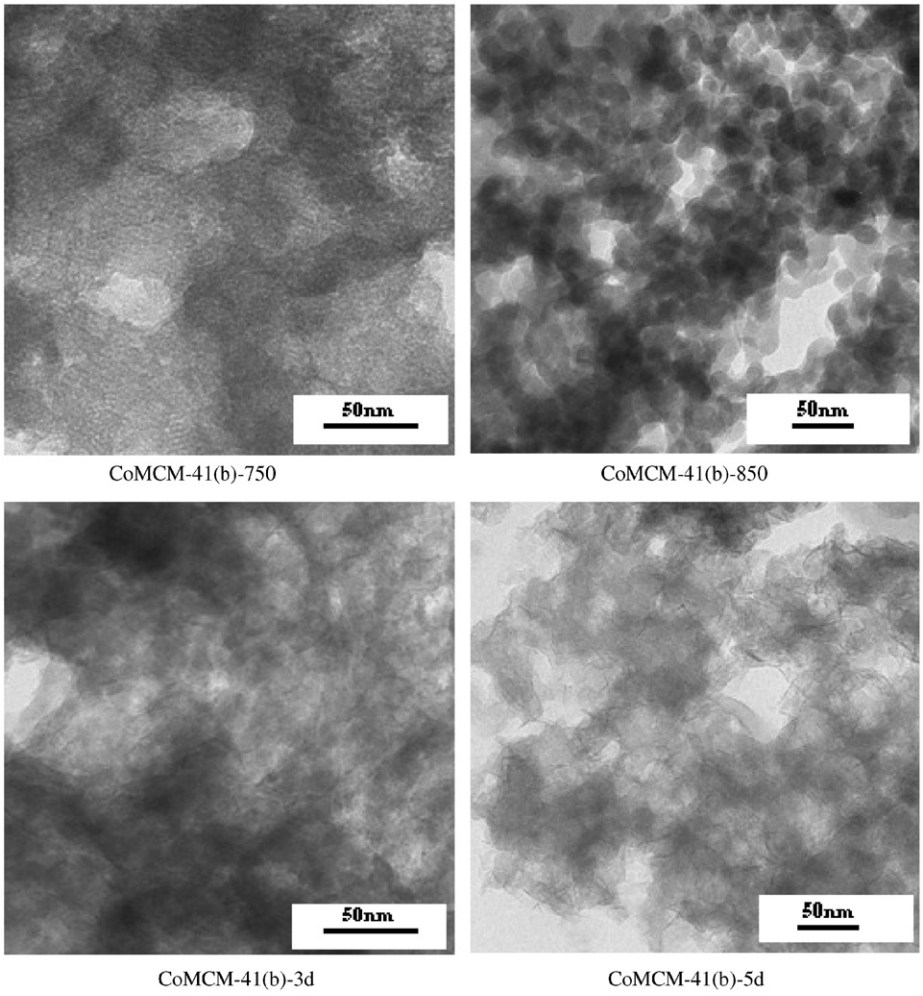

Fig. 2. TEM images of the synthesized CoMCM-41(b) sample after thermal or hydrothermal treatment.

by the Barrett–Joyner–Halenda (BJH) method [39]. The temperature programmed reduction (TPR) of the samples was carried out with a TP-5000 adsorption instrument (Tianjin Xianquan Corporation, China). First, 0.50 g of sample with particle sizes in the range of 250–425 μm was placed in the reactor, heated at a rate of 10 °C/min from room temperature to 400 °C and kept at 400 °C for 1 h in a flow of N_2. Then the sample was cooled to room temperature and reduced at a rate of 10 °C/min to 800 °C in a flow of N_2/H_2 (5 vol% H_2) mixture. The TPR profiles of the samples were recorded with a thermal conductivity detector. The cobalt contents of the synthesized samples were determined by inductive coupled plasma (ICP) technique (Vista-MAX, Varian). Transmission electron microscopy (TEM) morphologies of samples were observed with a Philips TEMCNAI-12 with an acceleration voltage of 100–120 kV.

3. Results and discussion

3.1. TEM analysis

Fig. 1 shows TEM images of the four samples after calcination at 550 °C. As shown in Fig. 1, all the four samples exhibit a hexagonal mesoporous structure of MCM-41 [1], and average pore sizes in the range 2.4–3.0 nm, showing that these samples have mesoporous structure and CoMCM-41 mesoporous molecular sieves were successfully synthesized under microwave irradiation. TEM images of the CoMCM-41(b) sample after thermal or hydrothermal treatment are illustrated in Fig. 2. From Fig. 2, we can observe that the CoMCM-41(b) sample still retains mesostructure after calcination at 750 °C for 3 h, but the mesoporous ordering decreases. When the CoMCM-41(b) sample was calcined at 850 °C for 3 h, the mesoporous framework was entirely damaged and the sample was transformed into fine grains. On the other hand, the CoMCM-41(b) sample has mesoporous

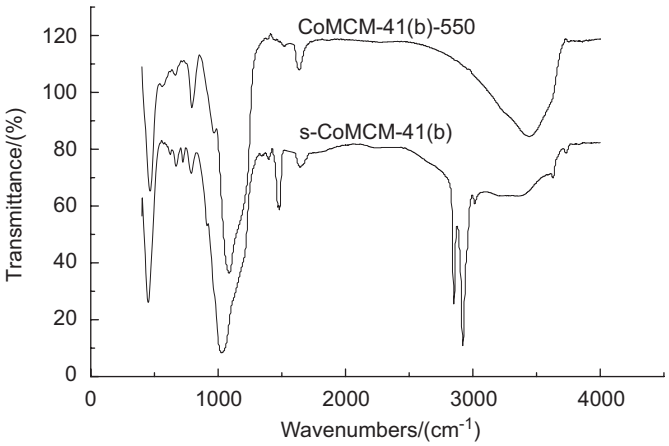

Fig. 4. FT-IR spectra of the CoMCM-41(b) sample synthesized according to the molar ratio of 1:0.2:0.10:70 (SiO_2:CTAB:CoO:H_2O). s-CoMCM-41(b), before calcination at 550 °C for 10 h; CoMCM-41(b)-550, after calcination at 550 °C for 10 h.

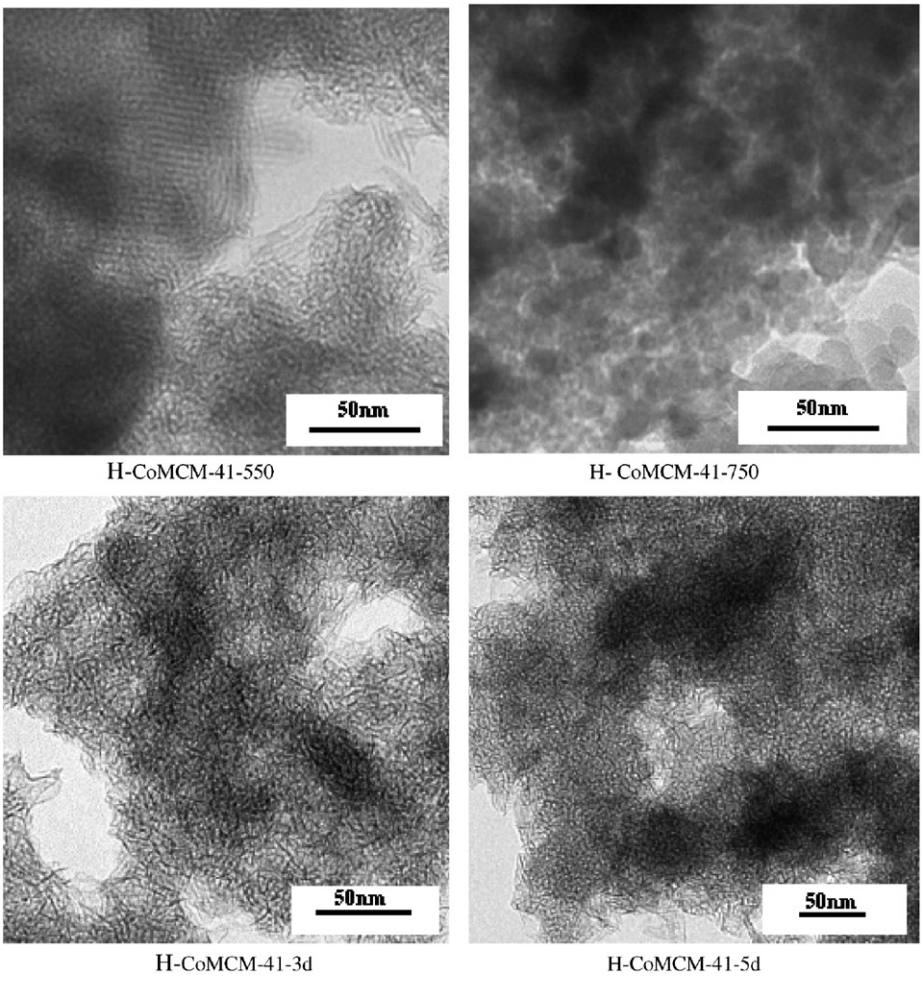

Fig. 3. TEM images of the synthesized H-CoMCM-41 sample after thermal or hydrothermal treatment.

framework after hydrothermal treatment at 100 °C for 3 or 5 days, but the mesoporous ordering decreases comparatively. The CoMCM-41(b) mesoporous molecular sieve was transformed into a wormhole-like structure. Fig. 3 presents TEM images of the H-CoMCM-41-550, H-CoMCM-41-750, H-CoMCM-41-3d and H-CoMCM-41-5d, respectively. As shown in Fig. 3, CoMCM-41 mesoporous molecular sieve was successfully synthesized by the conventional hydrothermal method. After the H-CoMCM-41 sample was calcined at 750 °C for 3 h, the mesoporous structure was mostly damaged. However, after the H-CoMCM-41 sample was hydrothermally treated at 100 °C for 3 or 5 days, the mesoporous framework was partly damaged. From Figs. 2 and 3, we can conclude that thermal stability of CoMCM-41 mesoporous molecular sieve synthesized by the microwave irradiation method is higher than that of CoMCM-41 mesoporous molecular sieve synthesized by the conventional hydrothermal method and that the hydrothermal stability is lower.

3.2. FT-IR analysis

FT-IR spectra of the CoMCM-41(b) sample before and after calcination at 550 °C are presented in Fig. 4. As shown in Fig. 4, the band at 3500 cm^{-1} is the characteristic band of the adsorbed water molecules; the bands at 2921, 2850 and 1480 cm^{-1} are the characteristic bands of the surfactant alkyl chains; the bands at 1620–1640 cm^{-1} are caused by the vibration of the adsorbed water molecules; the band at 1050 cm^{-1} is from the vibration of Si–O–Si. From Fig. 3, the bands at 2921, 2850 and 1480 cm^{-1} disappeared after the s-CoMCM-41(b) sample was calcined at 550 °C for 10 h, but the other characteristic bands did not disappear, which shows that the template has been effectively removed. Furthermore, a weak band at 960 cm^{-1} ascribed to the vibration of Co–O–Si was observed, indicating that cobalt ions were coordinated in the pore walls of the synthesized mesoporous molecular sieve [17].

3.3. XRD analysis

Fig. 5 shows the small-angle XRD patterns of the four samples after calcination at 550 °C for 10 h. As can be seen from Fig. 5, all the calcined samples have a diffraction peak (100) at 2θ value of ca. 2.3°, and have small and weak diffraction peaks at 2θ value ranging from 3° to 7° consistent with the characteristic diffraction patterns of the typical MCM-41 mesoporous molecular sieve [1], indicating that the samples synthesized under microwave irradiation have typical hexagonal mesoporous structure of MCM-41. Furthermore, as certified by XRD and TEM analyses, CoMCM-41 mesoporous molecular sieves with hexagonal arrangement were successfully synthesized. Additionally, from Fig. 5, the first diffraction peak in CoMCM-41(a) related to the (100) plane exhibits the highest intensity among all the samples. The diffraction peak (100) becomes weak and broad with the increase of the amount of cobalt added, indicating that the long-range ordering of the synthesized sample decreases with the increase of the amount of cobalt added, which agrees with the results from Bhoware et al. [17]. It is reasonable to conclude that the mesoporous ordering of the synthesized sample decreases with the increase of the amount of cobalt added in mesoporous molecular sieve.

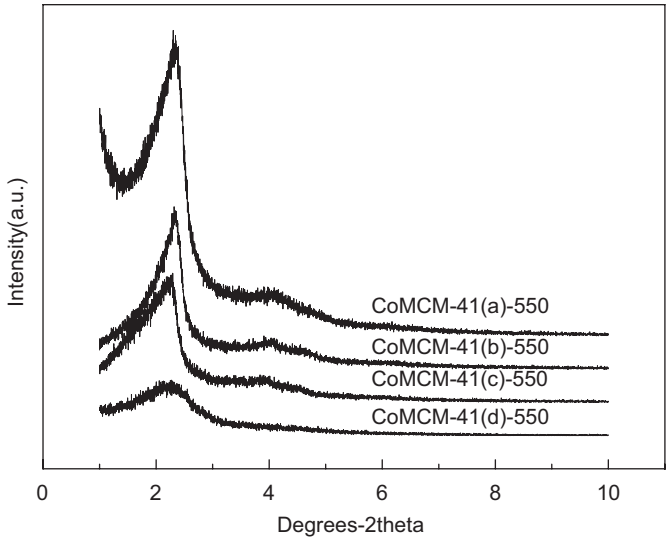

Fig. 5. XRD patterns of the samples synthesized according to the different molar ratios of SiO_2:CTAB:CoO:H_2O. CoMCM-41(a), CoMCM-41(b), CoMCM-41(c) and CoMCM-41(d) samples were calcined at 550 °C for 10 h, respectively.

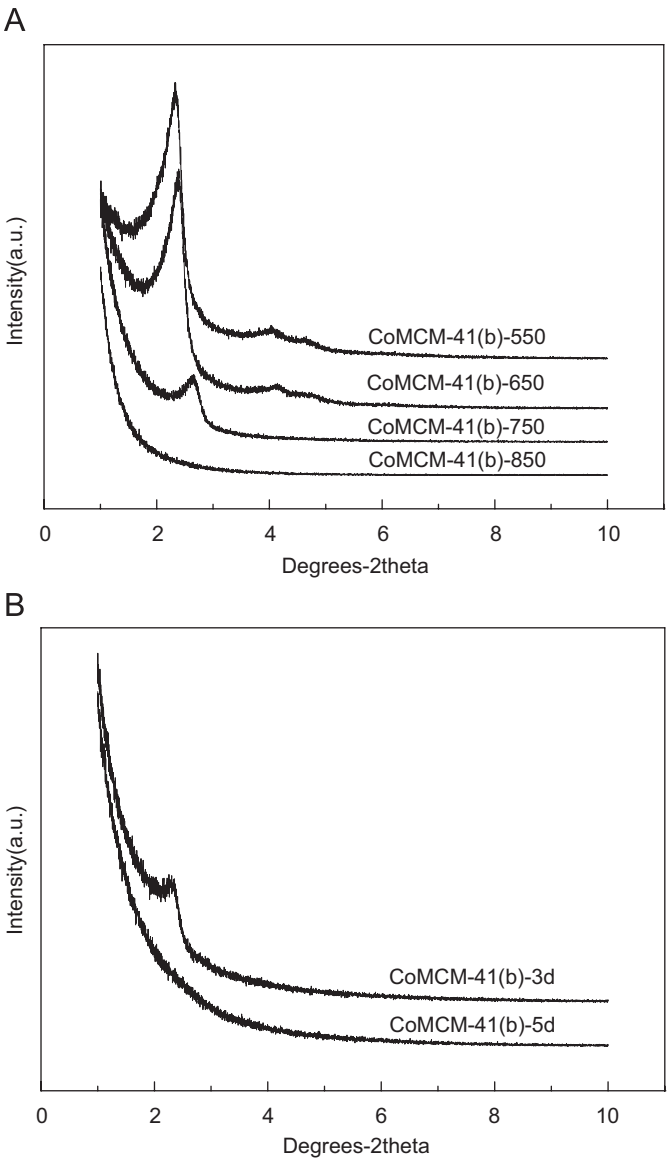

Fig. 6. XRD patterns of the CoMCM-41(b) sample synthesized according to the molar ratio of 1:0.2:0.10:70 (SiO_2:CTAB:CoO:H_2O). (A) After thermal treatment at 550, 650, 750 and 850 °C for 3 h, respectively; (B) after hydrothermal treatment at 100 °C for 3 or 5 days.

The small-angle XRD patterns of the CoMCM-41(b) sample after thermal and hydrothermal treatment are shown in Fig. 6. The XRD patterns of the other samples are similar to those of CoMCM-41(b). d_{100} calculated by the formula $2d_{100}\sin\theta = n\lambda$ and the unit cell parameters calculated by the formula $a_0 = 2d_{100}/\sqrt{3}$ are listed in Table 2. As shown in Fig. 6A, the CoMCM-41(b) sample still has diffraction peak (100) after calcination at 650 °C for 3 h, and the intensity of diffraction peak (100) is both strong and sharp, showing that the CoMCM-41(b)-650 has good mesoporous ordering, uniform pore distribution and large pore volume. In addition, from Fig. 6A, although we can observe that the peak (100) obviously exists after the CoMCM-41(b) sample was calcined at 750 °C for 3 h, the peak (100) becomes weak and broad, indicating that the CoMCM-41(b)-750 still retains the mesoporous framework, but the mesoporous ordering decreases. However, after the CoMCM-41(b) sample was calcined at 850 °C for 3 h, the diffraction peak (100) disappeared, showing that the mesoporous framework was entirely damaged. Additionally, as can be seen from Fig. 6A, the diffraction peak (100) shifted to a higher 2θ value with the rise of the calcination temperature, showing that d_{100} and a_0 values of the synthesized CoMCM-41 sample decrease and the pore size shrinks, which is consistent with the data of pore size listed in Table 2. On the other hand, from Fig. 6B, the CoMCM-41(b) sample still has the diffraction peak (100) after hydrothermal treatment at 100 °C for 3 days, certifying that the mesoporous framework still remains. However, after the CoMCM-41(b) sample was hydrothermally treated at 100 °C for 5 days, the diffraction peak (100) disappeared, indicating that the mesoporous framework was entirely collapsed.

3.4. Nitrogen adsorption

The N_2 adsorption–desorption isotherms and pore size distribution curves of the synthesized samples after calcination at 550 °C are shown in Fig. 7. Fig. 8 illustrates the N_2 adsorption–desorption isotherms of the synthesized CoMCM-41(b) sample after thermal treatment at different temperatures (550, 650, 750 and 850 °C, respectively), or hydrothermal treatment at different time (3 and 5 days, respectively). The specific surface areas, pore size distributions and pore volumes are listed in Table 2. As shown in Fig. 7A, we can observe that all isotherms exhibit typical type IV isotherms with hysteresis loop caused by capillary condensation in mesopores, certifying that all the samples have mesoporous structure. From Fig. 7A, all the isotherms exhibit a sharp step at a relative pressure of ca. 0.3–0.4, further showing that all the samples have typical mesostructure with uniform pore size distribution and large pore volumes [1]. Moreover, we can observe that the N_2 adsorption–desorption isotherms of the samples exhibit a sharp step at a relative pressure of ca. 0.9 in Fig. 7A, which is probably attributed to interparticle pores in samples. In addition, the isotherms of the CoMCM-41(a)-550 sample exhibit a sharp step as compared with the others samples, indicating that CoMCM-41(a)-550 have more uniform pore size distribution. Additionally, as shown in Fig. 7B, the narrow and sharp peaks can be observed in an average pore size range of 2.4–2.7 nm, further indicating that the samples have uniform pore size distribution after calcination at 550 °C. Furthermore, from Fig. 7B, all the samples have two types of mesopores with different pore sizes of ca. 2.5 and 4.0 nm, respectively. The pores with an average pore size of ca. 2.5 nm are dominant. The pores with an average pore size of ca. 4.0 nm are probably attributed to the interparticle pores present in samples. A sharp step present at a relative pressure of ca.0.9 in the isotherms also confirms the above conclusion. On the other hand, as shown in Fig. 8A, while the synthesized CoMCM-41(b) sample was calcined at 650 °C, the N_2 adsorption–desorption isotherms exhibit typical type IV isotherms, showing that the CoMCM-41(b)-650 sample has uniform pore size distribution and large pore volume. However, the N_2 adsorption–desorption

Table 2
Analyses of XRD, specific surface areas and pore sizes of the synthesized samples

Samples	a_0/nm	d_{100}/nm	Surface area/ ($m^2\,g^{-1}$)	BET constants	Average pore size/nm	Pore volume/ ($cm^3\,g^{-1}$)
CoMCM-41(a)-550	4.28	3.71	1189	41.9	2.46	1.02
CoMCM-41(b)-550	4.35	3.78	1031	58.5	2.55	0.98
CoMCM-41(c)-550	4.40	3.81	805	46.1	2.72	0.93
CoMCM-41(d)-550	4.55	3.94	746	71.2	2.75	0.75
CoMCM-41(a)-650	4.26	3.69	767	33.7	2.44	0.77
CoMCM-41(b)-650	4.26	3.69	645	47.6	2.45	0.76
CoMCM-41(c)-650	4.25	3.68	589	34.5	2.46	0.60
CoMCM-41(d)-650	4.51	3.90	451	72.4	2.47	0.66
CoMCM-41(a)-750	3.75	3.24	274	89.3	1.71	0.52
CoMCM-41(b)-750	3.88	3.36	268	62.5	1.71	0.52
CoMCM-42(c)-750	4.04	3.50	255	28.1	1.92	0.31
CoMCM-41(d)-750	4.19	3.63	223	58.3	1.28	0.41
CoMCM-41(a)-850	–	–	93	269.3	7.81	0.22
CoMCM-41(b)-850	–	–	94	199.5	6.94	0.21
CoMCM-41(c)-850	–	–	72	384.6	3.85	0.17
CoMCM-41(d)-850	–	–	99	140.3	6.51	0.25
CoMCM-41(a)-3d	4.30	3.72	381	232.4	3.80	0.44
CoMCM-41(b)-3d	4.50	3.90	326	203.2	3.42	0.50
CoMCM-41(c)-3d	4.40	3.81	275	167.3	3.91	0.37
CoMCM-41(d)-3d	4.47	3.87	270	261.8	3.40	0.51
CoMCM-41(a)-5d	–	–	311	123.4	3.81	0.44
CoMCM-41(b)-5d	–	–	279	109.1	3.39	0.49
CoMCM-41(c)-5d	–	–	251	124.8	3.41	0.41
CoMCM-41(d)-5d	–	–	224	108.3	0.92	0.45
H-CoMCM-41-550	4.27	3.65	908	39.8	2.52	0.96
H-CoMCM-41-650	4.08	3.60	617	30.5	2.41	0.75
H-CoMCM-41-750	–	–	194	85.7	6.73	0.34
H-CoMCM-41-3d	4.56	3.92	471	149.6	3.38	0.62
H-CoMCM-41-5d	–	–	389	320.9	3.40	0.53

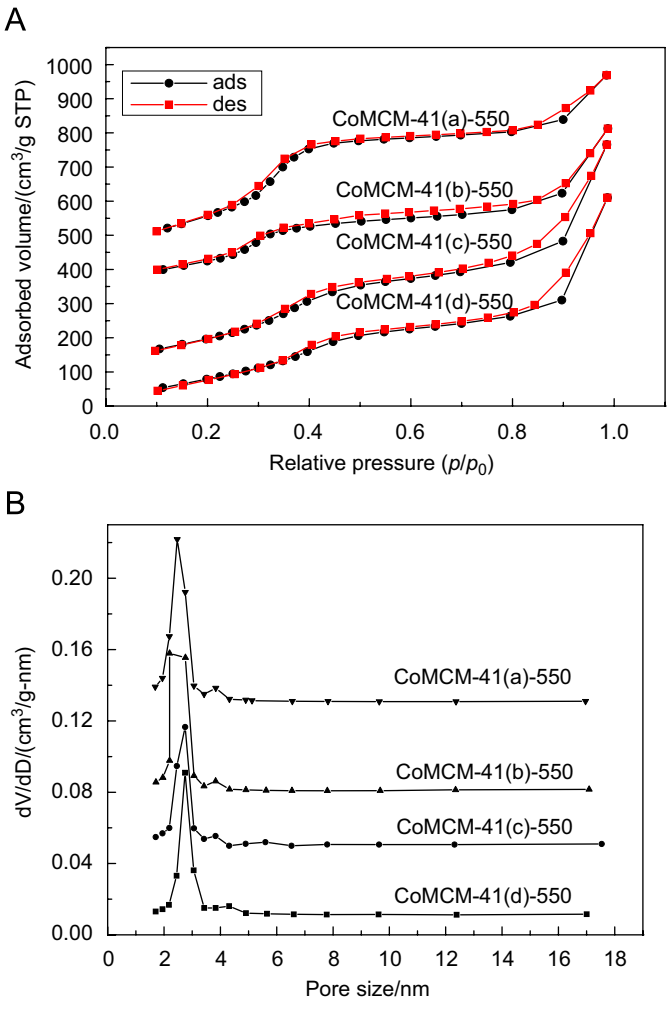

Fig. 7. (A) Nitrogen adsorption–desorption isotherms of the synthesized samples after calcination at 550 °C for 10 h; (B) pore size distribution curves of the synthesized samples after calcination at 550 °C for 10 h.

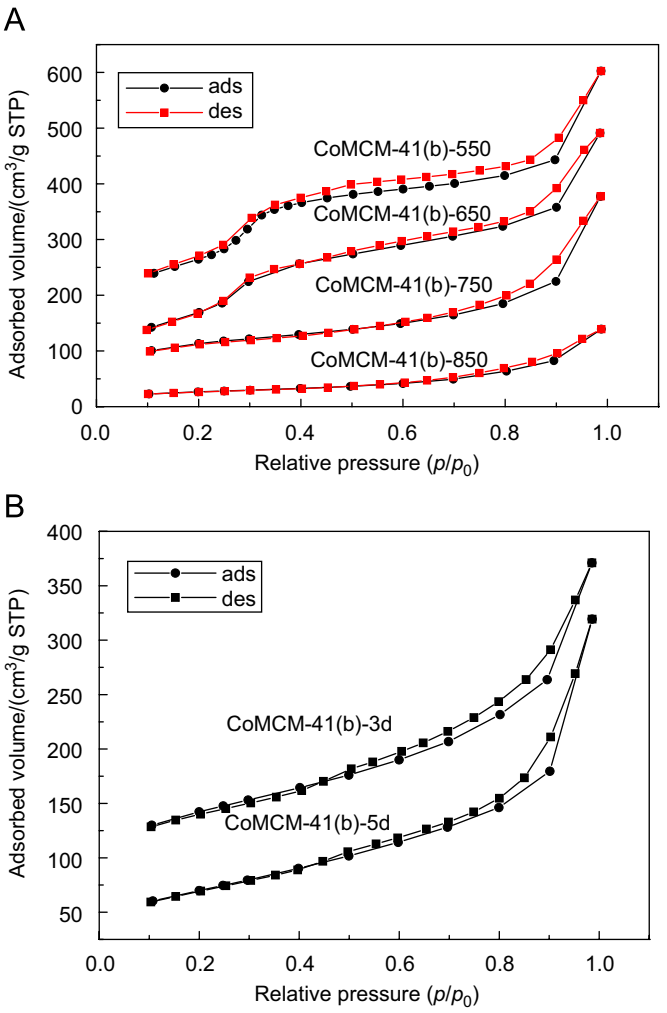

Fig. 8. Nitrogen adsorption–desorption isotherms of the CoMCM-41(b) sample synthesized according to the molar ratio of 1:0.2:0.10:70(SiO_2:CTAB:CoO:H_2O). (A) After thermal treatment at 550, 650, 750 and 850 °C for 3 h, respectively; (B) after hydrothermal treatment at 100 °C for 3 or 5 days.

isotherms of the CoMCM-41(b) sample do not exhibit obvious type IV isotherms after calcination at 750 °C for 3 h or hydrothermal treatment at 100 °C for 3 days. Combined with the results of XRD analysis, the CoMCM-41(b)-750 or CoMCM-41(b)-3d sample has mesoporous framework, but the pore size distribution is not uniform and the pore volume is small, which indicates that the mesoporous ordering decreases and the mesoporous framework was partly damaged.

From Table 2, the specific surface areas and pore volumes of all the samples synthesized by the microwave irradiation method after calcination at 550 °C decreases with the increase of the amount of cobalt added in starting materials. Combined with the results of XRD and N_2 adsorption–desorption isotherms, it is reasonable to conclude that the ordering of the synthesized mesoporous molecular sieves decreases with the increase of the amount of cobalt added. Additionally, the specific surface areas and pore volumes of these samples also decrease with the rise of the calcination temperature or the prolonging of hydrothermal treatment time. Moreover, the specific surface area and pore volume of the CoMCM-41(b) sample after calcination at 850 °C are very small, indicating that the mesoporous framewok has been entirely collapsed. On the other hand, the specific surface area and pore volume of the CoMCM-41(b) sample after hydrothermal treatment at 100 °C for 5 days greatly

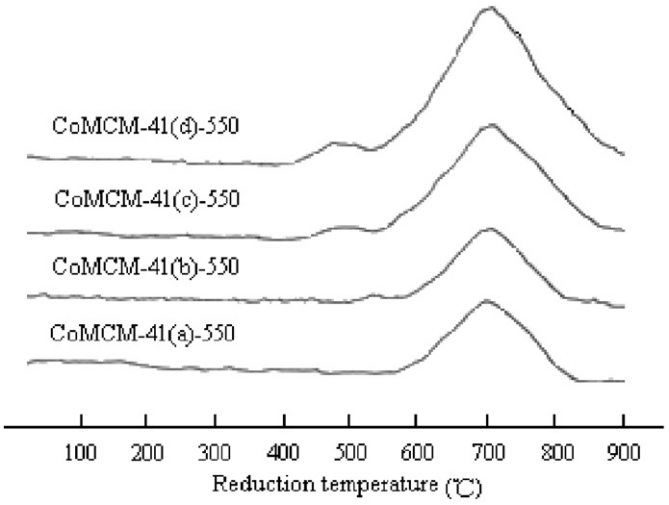

Fig. 9. TPR profiles of the synthesized samples after calcination at 550 °C.

decreased, showing that the mesoporous framework was partly damaged. In addition, as shown in Table 2, CoMCM-41 mesoporous molecular sieves have specific surface areas in a range of

746–1189 m^2/g and average pore size in a range of 2.46–2.75 nm. Furthermore, as shown in Table 2, the specific surface area of the H-CoMCM-41sample after calcination at 750 °C for 3 h is lower than that of CoMCM-41(b)-750. On the other hand, the specific surface area of the H-CoMCM-41sample after hydrothermal treatment at 100 °C for 3 or 5 days is higher than that of CoMCM-41(b)-3d or CoMCM-41(b)-5d. Combined with the analysis of TEM, it is reasonable to conclude that the thermal stability of the CoMCM-41 synthesized by the microwave irradiation method is higher than that of the CoMCM-41 synthesized by the conventional hydrothermal method, but hydrothermal stability is lower than that of the CoMCM-41 by the conventional hydrothermal method.

3.5. TPR analysis

Fig. 9 displays TPR profiles of the four samples after calcination at 550 °C. According to literatures [23,40,41], the reduction temperatures of cobalt ions supported by MCM-41 are in a range of 300–500 °C, but the reduction temperatures of cobalt ions coordinated in the pore walls of MCM-41 ranged from 700 to 800 °C. Fig. 9 shows that strong reduction peaks appear at about 700 °C and that weak reduction peaks appear at about 400–500 °C with the increase of the cobalt content. It is reasonable to conclude that cobalt ions were dominantly coordinated in the mesoporous framework, and that small amount of surface-located cobalt appeared only at a high cobalt content.

4. Conclusions

Well-ordered hexagonal CoMCM-41 mesoporous molecular sieves with different amounts of cobalt have been successfully synthesized by the microwave irradiation method. The synthesized samples were calcined at 550 °C for 10 h, and the template was effectively removed. The specific surface areas and pore volumes of the synthesized mesoporous molecular sieves decrease with the increase of the amount of cobalt added, and the mesoporous ordering also decreases. On the other hand, the mesoporous framework of the synthesized CoMCM-41 mesoporous molecular sieve still retained after calcination at 750 °C. However, after hydrothermal treatment at 100 °C for 5 days, the ordering of the synthesized CoMCM-41 mesoporous molecular sieve greatly decreased, and was transformed into the wormhole-like structure. When the addition of cobalt in the starting material is 0.05 mol, the mesoporous ordering of the synthesized sample is the best among the four doping contents. The thermal stability of CoMCM-41 mesoporous molecular sieve synthesized under microwave irradiation was enhanced as compared with that of CoMCM-41 mesoporous molecular sieve obtained by the hydrothermal method.

Acknowledgments

The authors are grateful to the financial support from Senior Personality Fund of Jiangsu University (06JDG074) and Industry Key Item Fund of Zhenjiang City (GY2006017)

References

[1] J.S. Beck, J.C. Vartuli, W.J. Roth, M.E. Leonowicz, C.T. Kresge, K.D. Schmitt, C.T.-W. Chu, D.H. Olson, E.W. Sheppard, S.B. McCullen, J.B. Higgins, J.L. Schlenkert, J. Am. Chem. Soc. 114 (1992) 10834.
[2] T.R. Gaydhankar, V. Samuel, P.N. Joshi, Mater. Lett. 60 (2006) 957.
[3] U.S. Taralkar, R.K. Jha, P.N. Joshi, J. Non-Crys. Solids 353 (2007) 194.
[4] J.O. Barth, A. Jentys, J. Kornatowski, J.A. Lercher, Chem. Mater. 16 (2004) 724.
[5] T. Jiang, Q. Zhao, H. Yin, Appl. Clay Sci. 35 (2007) 155.
[6] E.F. Iliopoulou, E.V. Antonakou, S.A. Karakoulia, I.A. Vasalos, A.A. Lappas, K.S. Triantafyllidis, Chem. Eng. J. 134 (2007) 51.
[7] N.B. Lihitkar, Majid Kazemian Abyaneh, V. Samuel, R. Pasricha, S.W. Gosavi, S.K. Kulkarni, J. Colloid Interface Sci. 314 (2007) 310.
[8] K. Okumura, K. Nishigaki, M. Niwa, Micropor. Mesopor. Mater. 44-45 (2001) 509.
[9] Q. Zhang, Y. Wang, Y. Ohishi, T. Shishido, K. Takehira, J. Catal. 202 (2001) 308.
[10] M. Florea, M. Sevinci, V.I. Pârvulescu, G. Lemay, S. Kaliaguine, Micropor. Mesopor. Mater. 44-45 (2001) 483.
[11] A. Corma, M.T. Navarro, L. Nemeth, M. Renz, Chem. Commun. 21 (2001) 2190.
[12] L. Noreña-Franco, I. Hernandez-Perez, J. Aguilar-Pliego, A. Maubert-Franco, Catal. Today 75 (2002) 189.
[13] K.M.S. Khalil, J. Colloid Interface Sci. 315 (2007) 562.
[14] S. Lim, D. Ciuparu, C. Pak, F. Dobek, Y. Chen, D. Harding, L. Pfefferle, G. Haller, J. Phys. Chem. B 107 (2003) 11048.
[15] Y. Chen, D. Ciuparu, S. Lim, G.L. Haller, L.D. Pfefferle, Carbon 44 (2006) 67.
[16] T. Somanathan, A. Pandurangan, D. Sathiyamoorthy, J. Mol. Catal. A 256 (2006) 193.
[17] S.S. Bhoware, A.P. Singh, J. Mol. Catal. A 266 (2007) 118.
[18] C.S. Song, K.M. Reddy, Appl. Catal. A 176 (1999) 1.
[19] J. Panpranot, J.G. Goodwin, A. Sayari, Catal. Today 77 (2002) 269.
[20] D. Ciuparu, Y. Chen, S. Lim, G.L. Haller, L. Pfefferle, J. Phys. Chem. B 108 (2004) 503.
[21] D. Ciuparu, Y. Chen, S. Lim, Y. Yang, G.L. Haller, L. Pfefferle, J. Phys. Chem. B 108 (2004) 15565.
[22] A. Jentys, N.H. Pham, H. Vinek, M. Englisch, J.A. Lercher, Catal. Today 39 (1998) 311.
[23] S.Y. Lim, D. Ciuparu, Y.H. Yang, G.A. Du, L.D. Pfefferle, G.L. Haller, Micropor. Mesopor. Mater. 101 (2007) 200.
[24] Q. Zhao, J. Chu, T. Jiang, H. Yin, Colloids Surf. A 301 (2007) 388.
[25] D. Subashini, A. Pandurangan, Catal. Commun. 8 (2007) 1665.
[26] V. Parvulescu, B.L. Su, Catal. Today 69 (2001) 315.
[27] H.T. Gomes, P. Selvam, S.E. Dapurkar, J.L. Figueiredo, J.L. Faria, Micropor. Mesopor. Mater. 86 (2005) 287.
[28] T. Jiang, Q. Zhao, H. Yin, J. Porous. Mater. 14 (2007) 457.
[29] Q. Qin, J. Ma, K. Liu, J. Colloid Interface Sci. 315 (2007) 80.
[30] P.B. Amama, S. Lim, D. Ciuparu, L. Pfefferle, G.L. Haller, Micropor. Mesopor. Mater. 81 (2005) 191.
[31] C.G. Wu, T. Bein, Chem. Commun. 8 (1996) 925.
[32] G.A. Tompsett, W.C. Conner, K.S. Yngvesson, Chem. Phys. Chem. 7 (2006) 296.
[33] C.S. Cundy, Collect. Czech Chem. Commun. 63 (1998) 1699.
[34] S.E. Park, D.S. Kim, J.S. Chang, W.Y. Kim, Catal. Today 44 (1998) 301.
[35] M. Bandyopadhyay, H. Gies, C. R. Chimie 8 (2005) 621.
[36] M.C.A. Fantini, J.R. Matos, L.C. Cides da Silva, L.P. Mercuri, G.O. Chiereci, E.B. Celer, M. Jaroniec, Mater. Sci. Eng. B 112 (2004) 106.
[37] Y.K. Hwang, J.S. Chang, Y.U. Kwon, S.E. Park, Micropor. Mesopor. Mater. 68 (2004) 21.
[38] K. Bachari, O. Cherifi, Catal. Commun. 7 (2006) 926.
[39] E.P. Barrett, L.G. Joyner, P.P. Halenda, J. Am. Chem. Soc. 73 (1951) 373.
[40] Q.H. Tang, Q.H. Zhang, H.L. Wu, Y. Wang, J. Catal. 230 (2005) 384.
[41] S.Y. Lim, Y.H. Yang, D. Ciuparu, C. Wang, Y. Chen, L. Pfefferle, G.L. Haller, Topics in Catal. 34 (2005) 31.